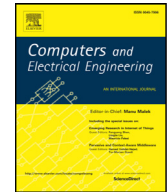




Contents lists available at ScienceDirect

## Computers and Electrical Engineering

journal homepage: [www.elsevier.com/locate/compeleceng](http://www.elsevier.com/locate/compeleceng)

# An image response framework for no-reference image quality assessment<sup>☆</sup>

Tongfeng Sun<sup>\*</sup>, Shifei Ding, Xinzheng Xu

School of Computer Science and Technology, China University of Mining and Technology, Xuzhou, Jiangsu 221116, China

## ARTICLE INFO

### Article history:

Received 22 April 2017

Revised 6 December 2017

Accepted 6 December 2017

Available online xxx

### Keywords:

No-reference image quality

Multi-scale preprocessing

Image input

Image object response

## ABSTRACT

This paper proposes an image response framework for no-reference image quality assessment (NR IQA). The framework is an image quality feature extension framework, extending existing image quality features to new NR image quality features. In the framework, a test image is transformed into a number of sub-images through multi-scale preprocessing. The sub-images are taken as image objects, and each object is exerted with multiple local convolution operations as image inputs. Object responses are extracted from the objects under the inputs based on existing image quality features. All the responses compose a global image response feature vector and are mapped to a quality index. Object responses are the NR extensions of the existing image quality features, which signifies the extensions of IQA approaches. Experiments show that the framework can extend full-reference IQA and reduced-reference IQA approaches to NR IQA approaches, and extend NR IQA approaches to new higher-performance NR IQA approaches.

© 2017 Elsevier Ltd. All rights reserved.

## 1. Introduction

An accurate quantitative index on the perception quality of an image is highly desirable in many application fields, such as image preprocessing, fusion, transmission and restoration. In most cases, images are eventually perceived by human beings, and therefore subjective quality assessment is the most "correct" method. But subjective assessment is expensive and time-consuming. Consequently, there is a significant need for objective approaches without human participations. According to the available information of non-distorted reference image in image quality assessment (IQA), objective IQA approaches are categorized into three groups: (1) full-reference (FR) approaches, (2) reduced-reference (RR) approaches and (3) no-reference (NR) approaches.

- (1) *FR approaches* assess the perceptual quality of a test image on an assumption that the reference image with the highest quality is available. Classic FR approaches mainly include mean square error (MSE) [1], peak signal-to-noise ratio (PSNR) [2], structure similarity index (SSIM) [3], etc. They assess the perceptual quality of a test image by calculating the similarity or difference between the test image and its reference image.
- (2) *RR approaches* access partial reference information instead of the full reference image. With RR approaches, such as WNISM [4] and RRED [5], the similarity or difference between the test image and its reference image also needs to

<sup>☆</sup> Reviews processed and recommended for publication to the Editor-in-Chief by Area Editor Dr. E. Cabal-Yepez.

<sup>\*</sup> Corresponding author.

E-mail address: [stfok@126.com](mailto:stfok@126.com) (T. Sun).

be calculated when assessing the quality of a test image. Thus, if the access to reference information is unavailable, neither FR nor RR approaches can work.

- (3) *NR approaches* assess image quality based on the test image itself without the access of the reference image [6–11]. Therefore, NR approaches have promising prospects. The research on NR approaches has been becoming a study focus in recent years.

With NR approaches, the most important problem is to extract the features which can fully depict image quality. Many early NR approaches are distortion-specific and they are only applicable to one or several specific types of distortions, such as blocking [6], ringing [7], blur [8], etc. The approaches probe into the mechanism of a special type of distortion, and assess image quality only if the distortion type is known in advance. Recently great efforts are devoted to the general-purpose (non-distortion-specific) NR approaches, which perform well for different types of distortions without the prior knowledge of distortion types. Natural scene statistics (NSS) models have been extensively studied and many NSS-model-based NR approaches have been proposed [9–21], which assume that natural scenes possess certain statistical properties and distortions will affect such properties. Gaussian scale mixture (GSM) model, Generalized Gaussian distribution (GGD) statistical model and asymmetric generalized Gaussian distribution statistical (AGGD) model are widely used NSS statistical models, which are important tools to depict image signal distributions and reveal the statistical characteristics of image signals [9–16]. The models can effectively model image spatial coefficients in NIQE [10] and BRISQUE [11], DCT coefficient in BLIINDS2 [12], wavelet coefficients in BIQI [13], curvelet coefficients in CURVELET [14], etc. Some of the NR approaches evenly outperform FR approaches under laboratory conditions. Among them, BIQI, CURVELET, BLIINDS2 and BRISQUE are opinion-aware approaches, which are trained on a database of distorted images and associated subjective opinion scores. NIQE is opinion unaware, which makes use of measurable deviations from statistical regularities observed in natural images to assess image quality, without training on human-rated distorted images. To improve the performance of some IQA approaches, much richer set of NSS features are deployed. BIQI proposed a two-step framework and assessed image quality by using the statistics of wavelet coefficients. It was extended to DIIVINE [9] by deploying a much richer set of NSS-based features: scale and orientation selective statistics, orientation selective statistics, correlations across scales, spatial correlation and across orientation statistics. NIQE predicts image quality by using the statistics of the spatial domain NSS. Inspired by it, IL-NIQE was proposed [16], which assessed image quality by adopting a variety of existing and new natural scene statistics (NSS) features: statistics of normalized luminance, statistics of MSCN products, gradient statistics, statistics of Log-Gabor filter response and statistics of colors. In [17, 18], Ye et al. established visual codebook models, based on which NR approaches called CB and CORNIA were proposed. In the NR approaches, a codebook is firstly constructed from the local features extracted based on training images. Then, the local features extracted from the test image are encoded as a vector through quantization according to the codebook. Finally, the image quality is assessed by mapping the vector to a quality index through a nonlinear regression. Gradient conveys rich information regarding image edges and structures and gradient models have been widely used in image recognition, image quality assessment, image registration, etc. In [19] and [20], Sun et al. and Liu et al. proposed NR approaches based on gradient models, called GHR and OG-IQA: the former employs gradient histogram variations under local transform inputs to assess image quality; the latter employs gradient orientation features to assess image quality.

Although NR approaches have made great progresses, efforts should still be made to reduce the gaps between subjective indexes and predicted indexes to meet the requirements of actual applications. In this paper, an image response framework for NR IQA is proposed. The framework is a general-purpose framework, different from the framework in [13, 18], which are restricted to some specific NR approaches for extracting NR features. In theory, the framework is applicable to all the existing IQA features, including the existing FR, RR and NR IQA features. Through the framework, the existing IQA features are extended to response features, which act as new NR IQA features. In other words, the existing IQA approaches, including FR, RR and NR IQA approaches, are extended to new NR IQA approaches. Therefore, the framework provides a NR-IQA production method, which will produce different NR approaches through deploying different image quality features. The rest of this paper is organized as follows. Section 2 introduces previous work, focusing on image quality feature extraction. In Section 3, an image response framework for NR quality assessment is proposed. Based on the framework, image preprocessing, image input and image response are investigated in detail. In Section 4, experiments are carried out to verify the framework's performance through the performance of new NR IQA approaches extended from some existing IQA approaches. Finally, conclusions are presented in Section 5.

## 2. Previous work

IQA approaches generally involve two phases: feature extraction and feature-learning-based quality assessment. The features of IQA approaches normally reflect the statistical characteristics of the image to be assess. According to the classification of IQA approaches, image quality features can be categorized into three classes: FR features, RR features and NR features, corresponding to FR approaches, RR approaches and NR approaches, respectively. FR/RR feature extractions need the full/partial reference information while NR feature extraction is based on the test image itself without any access to reference image. Feature-learning-based quality assessment maps the features to quality indexes through some algorithmic models, such as probabilistic prediction [12], support vector regression (SVR) [10, 18], deep learning [15], etc. Obviously,



**Fig. 1.** Image response model.

feature extraction plays a vital role and the performances of IQA approaches mainly rely on the perceptual relevance of the extracted features. It is indispensable to attach importance to feature extraction in the investigation of IQA.

According to the role of human visual system (HVS) in feature extraction, the investigation methods of IQA can be classified into three categories:

- (1) *The category based on statistical characteristics of natural images:* statistical characteristics/features are extracted through data statistic algorithmic models based on training natural image data. During the feature extraction, HVS is not or little taken into account. Consequently, the key problem is to capture statistical features with high correlation with human perception quality. For example, PSNR used as FR feature is a statistic of the errors between the distorted image and its corresponding reference image; Generalized Gaussian distribution (GGD) statistical models is widely used to depict image data distribution in RR and NR approaches and the parameters of model are used for IQA [10, 22]; The codebook model used in CORNIA [18] encodes test images through quantization according to an advancedly-designed codebook, and the encoded features applied to NR IQA depict the statistical characteristics of the test image.
- (2) *The category based on HVS (human visual system):* The vital task of the category is to deeply investigate the properties and cognitive mechanism of HVS. Obtained on physiology and psychophysics experiments, it is found that the perception procedure of HVS consists of multi-channel sensation, just noticeable blur, and the contrast sensitivity function, etc. And HVS is sensitive to image structure, edge, contour, normalized color error, etc. These characteristics can be used in IQA investigation. For example, through modeling the procedure of HVS, Wang et al. proposed HVS-based fundus image quality assessment of portable fundus camera photographs [23]. Founded on the sensitivity to structural information in HVS, Wang et al. [3] proposed the SSIM IQA approach. In the light of the fact that HVS can tolerate the blur around an edge up to a certain threshold, a just noticeable blur method was proposed to blindly evaluate the perceptual sharpness [24]. Owing to the rich information that gradient conveys regarding image edges and structures, Sun et al. and Liu et al. proposed GHR [19] and OG-IQA [20] NR approaches.
- (3) *The category combining natural images statistical characteristics and HVS:* There is a popular trend of taking both natural image statistical characteristics and HVS into account in IQA approaches. The combination of them can produce new higher-performance IQA approaches. For example, Zhang et al. proposed a feature-enriched completely blind image quality, called IL-NIQE [16], which extract the IQA features: statistics of normalized luminance, statistics of MSCN (mean subtracted and contrast normalized coefficients) products, gradient statistics, statistics of Log-Gabor filter response and statistics of colors. Each feature can be looked as the combination of natural images statistical characteristics and HVS. In fact, even the IQA approaches based on statistical characteristics of natural images will more or less take HVS into account. For an instance, Mittal et al. proposed NIQE approach [10], which is based on the GGD model of natural scene statistic. However, in the patch selection of NIQE, only those patches with suprathreshold sharpness greater than a threshold  $T$  are selected to extract build models. It is due to a fact that humans appear to more heavily weight their judgments of image quality from the sharp image regions and more salient quality measurements can be made from sharp patches. However, because more attention is paid to NSS model, NIQE is divided into the first category.

Different with above three categories, NR IQA in this paper is implemented through feature extension. The purpose of the framework is not to investigate new features. It is inspired by a response-based investigation of unknown objects in the real world. Through the framework, the existing IQA features, which include FR, RR and NR features, are extended to response features—NR IQA features. That also means that the existing IQA approaches, which include FR, RR and NR IQA approaches, are extended to new NR IQA approaches.

### 3. Image response framework for NR image quality assessment

In the real world, the objects with different essential properties often response differently to the same stimulus inputs and their properties can be acquired by analyzing their responses. The response-based object investigation is a commonly-confronted instance. A common approach is to exert external stimuli as inputs to the object, and probe into its intrinsic essential property through analyzing its response outputs [25–27]. For example, in control field, the transfer function of a controlled object can be investigated according to its impulse response and step response; in software design field, a new software is an investigated object and its reliability and stability can be assessed through the analysis of its output responses under different application inputs; in medical field, a patient is an investigated object and his pathologies may be diagnosed according to its physiological responses under some physical stimuli. If a test image to be assessed is taken as an object, an image response model is put forward, as shown in Fig. 1. The model exerts external inputs to the object, and assesses the quality of the image object based on its response outputs.

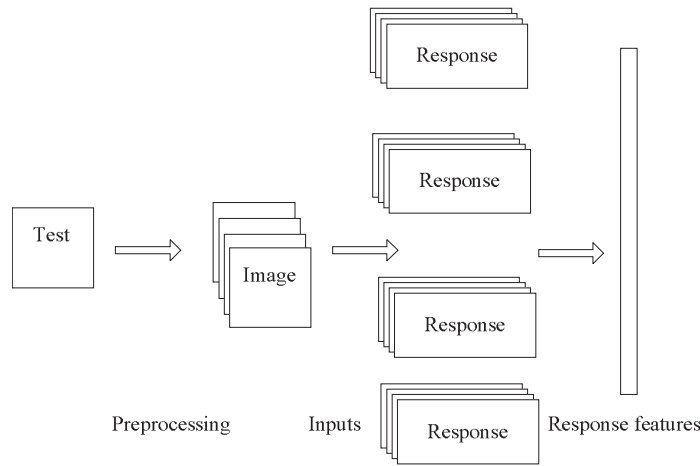


**Fig. 2.** Image response framework for NR image quality assessment.

As is known, multiscale space analysis has been widely used in the researches on high-dimension complex data. Images are naturally multiscale, and some IQA approaches have been proposed based on multiscale-space features [12, 28]. Here, the multiscale image space is set up through low-pass filtering with rotationally symmetric discrete Gaussian filters. Then, the test image is transformed into a number of sub-images. The multiscale-space transformation plays a role of image pre-processing. The sub-images instead of the test image are taken as image objects to produce response outputs. If each image object is exerted with multiple different inputs, a series of responses will be produced. So, an image response framework for NR image quality assessment is shown as Fig. 2. Through multiscale-space preprocessing, the test image to be assessed is firstly transformed into a number of sub-images, which are taken as image objects. Then, each object is exerted with multiple inputs, and a series of responses are produced. Each response corresponds to one image object and one input. In the condition that a image object is exerted with an input, the image object have two states: original image object (before being exerted with the input) and output image object (after being exerted with the input). The output image object is generated from the original image object under the input. The corresponding response output is the feature extracted from the two image objects. In Fig. 2, as an example, the test image is transformed into 4 image objects and each image object is exerted with 4 inputs. The 16 response features compose a global image response feature vector and are eventually mapped to a quality index. From the figure, it can be seen that there are at least three problems with the framework to revolve: image preprocessing, image inputs and response feature extraction.

### 3.1. Image preprocessing

Image preprocessing is to transform the test image into multiscale-space sub-images, namely, multiscale-space image objects. The sub-images of different scales have different minutiae properties, such as structure, edges, texture, etc. which are perceptually relevant. Multiscale Gaussian filtering is a frequently used multiscale analysis method. It is achieved through a convolution operation of a variable-scale Gaussian function  $G(x, y, \sigma)$  with a test image  $I(x, y)$ , as follows:

$$I_o = I(x, y) * G(x, y, \sigma) \quad (1)$$

$$G(x, y, \sigma) = \frac{1}{\sigma \sqrt{2\pi}} e^{-\frac{(x+y)^2}{2\sigma^2}} \quad (2)$$

where  $*$  is a convolution operation,  $I_o(x, y)$  is an image object and  $\sigma$  is a smoothing scale. Different scales correspond to different image objects. In image digital processing fields, Eq. (2) must be discretized into a  $N \times N$  matrix ( $N$  is a integer greater than 1) to meet the needs of discrete data processing. Then, Eq. (1) is changed into a discrete form:

$$I_o = I(x, y) * M \quad (3)$$

where  $M$  is a discrete preprocessing matrix of  $G(x, y, \sigma)$ . The matrix play a role of image blurring and its inverse operation apparently play a role of image enhancement. To distinguish the role of the matrix, it is labeled as  $M_b$ . Then, a Gaussian enhancement matrix  $M_e$  can be generated from  $M_b$ , given by

$$M_e = U + (U - M_b) = 2 \times U - M_b \quad (4)$$

where  $U$  is a preserving  $N \times N$  matrix, whose role is to preserve the original contents of  $I(x,y)$  in convolution operation. As an example with  $N$  equal to 3, its central element is 1 and other elements are 0, as in Eq. (5).

$$U = \begin{bmatrix} 0 & 0 & 0 \\ 0 & 1 & 0 \\ 0 & 0 & 0 \end{bmatrix} \quad (5)$$

### 3.2. Image inputs

HVS is sensitive to local image information, such as edge, structure, gradient and texture. Therefore, local image convolution operations are adopted as image inputs to change the local information of an image object. Response features as response outputs convey the local information of the image objects, and the response features of all the image objects are further used to assess the quality of the test image. In the framework, an image input is defined as

$$B = U + \eta A \quad (6)$$

where  $U$  is a preserving  $N \times N$  matrix, defined as in Eqs. (4) and (5), and  $A$  represents a basic image input unit.  $A$  is also a  $N \times N$  matrix, where the sum of all the elements is equal to 0, namely,  $\sum_{ai < n, < 1j < n} A_{i,j} = 0$ .  $\eta$  is an intensity coefficient, representing an input intensity. The image input  $B$  is exerted to a sub-image object as follows:

$$I^t(X, Y) = I_o(x, y) * B \quad (7)$$

where  $I_o(x,y)$  is an image object and  $*$  is a convolution operation. The basic image input units  $A$  can be roughly classified into image smoothing and image enhancement according to their effects on the local correlation of neighboring pixels in the image object. In the framework, the basic input unit is defined in two forms:

$$A = \begin{bmatrix} 0 & -0.25 & 0 \\ -0.25 & 1 & -0.25 \\ 0 & 0.25 & 0 \end{bmatrix} \quad (8)$$

$$A = \begin{bmatrix} -0.125 & -0.125 & -0.125 \\ -0.125 & 1 & -0.125 \\ -0.125 & -0.125 & -0.125 \end{bmatrix} \quad (9)$$

The two operators are two Laplacian operators, both playing a role of image enhancement. When  $\eta > 0$ ,  $B$  plays a role of image enhancement; when  $\eta < 0$ ,  $B$  plays a role of image blurring; when  $\eta = 0$ ,  $B$  has no effect on the image object.

### 3.3. Response features and image quality assessment

The extraction of response features is a key component of the framework. The new NR IQA is implemented based on the response features. The framework is an IQA feature extension framework, which extends existing IQA features to new NR IQA features. The existing IQA features are driven from existing IQA approaches, including FR, RR and NR approaches. In this way, the IQA approaches are extended to new NR IQA approaches. In the case that the existing IQA approach has more than one feature item, all the feature items are taken as a feature. It is generally known that each IQA approach is based on his own distinct feature, which is more or less different with those of other IQA approaches. Consequently, there is an one-to-one relationship between the existing IQA features and the existing IQA approaches.

With a FR feature, the feature is extracted by calculating the similarity or difference between the test image and its reference image. Namely, the extraction of the feature needs two images: the test image and the reference image. In view of this, if the original image object and its output image object (the image object under an image input) in the response framework are taken as a reference image and a test image respectively, the FR feature will be extracted. The FR feature as the response feature is used for IQA. As discussed in Section 3.1, multiscale-space preprocessing transforms a test image into a number of image objects. Simultaneously, each image object is exerted with multiple inputs and produces a series of response features. All the features compose a global vector and are mapped to a quality index. If the test image is transformed into  $n$  image objects (sub-images) and each image object is exerted with  $m$  inputs, the quality of the test image is assessed as follows:

$$F = [f_{o,1}, f_{o,2}, \dots, f_{o,i}, \dots, f_{o,n}] \quad (10)$$

$$f_{o,i} = [fr_{o,i}^1, fr_{o,i}^2, \dots, fr_{o,i}^j, \dots, fr_{o,i}^m] \quad (11)$$

$$fr_{o,i}^j = fr(I_{o,i}^j(x, y), I_{o,i}(x, y)) \quad (12)$$

$$Map(F) = index \quad (13)$$

In Eq. (10),  $F$  denotes a global feature vector of the test image, and  $f_{o,i}$  denotes the response features of the  $i$ th image object  $I_{o,i}(x, y)$ .  $F$  is composed of the response features of the  $n$  image objects. Because each object is exerted with  $m$  image inputs,  $f_{o,i}$  further consists of  $m$  elements as in Eq. (11). Each element  $fr_{o,i}^j$  is calculated through  $fr(I_{o,i}^j(x, y), I_{o,i}(x, y))$ , denoting the response feature for the  $i$ th object under the  $j$ th input.  $fr(I_{o,i}^j(x, y), I_{o,i}(x, y))$  in Eq. (12) represents the feature-extraction function of the FR feature. Finally, the global feature vector  $F$  is mapped to a quality index through a nonlinear regression as in Eq. (13). In this way, IQA is achieved. Because the IQA actually does not need any access to the corresponding reference image of the test image, a new NR approach is produced and the FR approach is extended to a new NR approach.

With a RR feature, the feature is extracted by calculating the similarity or difference based on the test image and the partial information of its reference image. If the image object and its output image object in the framework are taken as a reference image and a test image respectively, the partial reference information can be extracted from the image object and the RR feature can be extracted. If the test image is transformed into  $n$  image objects, the features of the  $n$  objects will also compose a global feature vector as in Eq. (10). Furthermore, if each object is exerted with  $m$  image inputs, the response feature  $f_{o,i}$  of the  $i$ th image object  $I_{o,i}(x, y)$  is as follows:

$$f_{o,i} = [rr_{o,i}^1, rr_{o,i}^2, \dots, rr_{o,i}^j, \dots, rr_{o,i}^m] \quad (14)$$

$$rr_{o,i}^j = rr(I_{o,i}^j(x, y), re_{o,i}) \quad (15)$$

In Eq. (14),  $rr_{o,i}^j$  denotes the response feature for the  $i$ th object under the  $j$ th input. It is calculated through  $rr(I_{o,i}^j(x, y), re_{o,i})$  in Eq. (15), where  $re_{o,i}$  is the partial reference information of the  $i$ th image object.  $rr(I_{o,i}^j(x, y), re_{o,i})$  represents the feature-extraction function of the RR feature. Finally, the global feature vector  $F$  is mapped to a quality index as in Eq. (13). In this way, the IQA feature is extracted without any access to the corresponding reference image of the test image. Namely, a new NR approach is produced and the RR approach is extended to a new NR approach.

With a NR feature, the feature is extracted based on the test image itself. It means that the feature can be extracted from the output image object. In addition, the NR feature of the original test image  $I(x, y)$  can be extracted based on itself and is used as one element of the global feature. Therefore, the global feature vector is as follows

$$F = [f, f_{o,1}, f_{o,2}, \dots, f_{o,i}, \dots, f_{o,n}] \quad (16)$$

$$f = nr(I(x, y)) \quad (17)$$

$$f_{o,i} = [nr_{o,i}^1, nr_{o,i}^2, \dots, nr_{o,i}^j, \dots, nr_{o,i}^m] \quad (18)$$

$$nr_{o,i}^j = nr(I_{o,i}^j(x, y)) \quad (19)$$

In (16),  $f$  demotes the feature extracted from the original test image, and  $f_{o,i}$  demotes the features of the  $i$ th object  $I_{o,i}(x, y)$ .  $f_{o,i}$  consists of  $m$  elements, among which  $nr_{o,i}^j$  is the feature extracted from the  $i$ th object under the  $j$ th input.  $nr(I(x, y))$  in Eq. (17) and  $nr(I_{o,i}^j(x, y))$  in Eq. (19) represent the feature-extraction function of the NR feature. The global feature vector is also mapped to a quality index by Eq. (13). In this way, the IQA feature is extracted without any access to the corresponding reference image of the test image. Namely, a new NR approach is generated and the NR approach is extended to a new NR approach.

#### 4. Experiments

The validity of the framework is verified by the performance of the new NR IQA approaches extended from the existing IQA approaches through the framework. Apparently, the new NR approaches extended from different IQA approaches (namely, based on different NR features) will show different performance. It is unnecessary to require that all the new approaches must outperform the state of art NR approaches. With regard to the new NR approaches extended from the FR and RR approaches, there is an improvement in IQA as long as the new approaches can perform well as NR approaches. The improvement indicates that the FR and RR approaches are successfully extended to new NR approaches and the validity of the framework is verified. With regard to the new NR approaches extended from the NR approaches, there is an improvement in IQA as long as they show relatively better performances compared with their corresponding original NR approaches. The improvement indicates that the NR approaches are successfully extended to new higher-performance NR approaches and the validity of the framework is verified.

Before carrying out the experiments, there are two problems that need to be resolved in advance.

- (1) *The first problem* is to choose some existing IQA approaches, which are extended to new NR approaches. It is impossible to choose all the existing IQA approaches in the experiments. The chosen IQA approaches include PSNR, SSIM [3], WNISM [4], RRED [5], NIQE [10], CURVELET [14], and CORNIA [18]. Among the approaches, the first two are FR



**Table 1**

The chosen IQA approaches for extension and the new corresponding NR approaches produced through the response framework.

Existing IQA approaches	New NR IQA approaches
PSNR, SSIM (FR approaches)	<b>PSNRR, SSIMR</b>
WNISM, RRRED (RR approaches)	<b>WNISM, RRREDR</b>
NIQE, CURVELET, CORNIA (NR approaches)	<b>NIQER, CURVELETR, CORNIAR</b>

**Table 2**

Median LCCs in the LIVE database.

	JP2K	JPEG	WN	BLUR	FF	ALL
PSNR	0.952	0.943	0.943	0.746	0.903	0.915
SSIM	0.967	0.965	0.939	0.906	0.947	0.940
NIQE	0.769	0.858	0.954	0.664	0.825	0.803
CURVELET	0.878	0.895	0.974	0.916	0.763	0.828
CORNIA	0.899	0.894	0.960	0.948	0.920	0.912
BIQI	0.874	0.724	0.981	0.917	0.827	0.777
BLIINDS2	0.961	0.973	0.974	0.942	0.925	0.922
BRISQUE	0.938	0.972	0.993	0.949	0.905	0.932
IL-NIQE	0.903	0.936	0.972	0.921	0.841	0.892
OG-IQA	0.946	0.983	0.990	0.967	0.911	0.952
<b>PSNRR</b>	<b>0.790</b>	<b>0.797</b>	<b>0.949</b>	<b>0.935</b>	<b>0.772</b>	<b>0.820</b>
<b>SSIMR</b>	<b>0.948</b>	<b>0.947</b>	<b>0.987</b>	<b>0.915</b>	<b>0.876</b>	<b>0.931</b>
<b>WNISM</b>	<b>0.721</b>	<b>0.570</b>	<b>0.816</b>	<b>0.888</b>	<b>0.767</b>	<b>0.752</b>
<b>RREDR</b>	<b>0.941</b>	<b>0.925</b>	<b>0.962</b>	<b>0.896</b>	<b>0.820</b>	<b>0.927</b>
<b>NIQER</b>	<b>0.970</b>	<b>0.960</b>	<b>0.980</b>	<b>0.953</b>	<b>0.925</b>	<b>0.962</b>
<b>CURVELETR</b>	<b>0.959</b>	<b>0.961</b>	<b>0.987</b>	<b>0.957</b>	<b>0.914</b>	<b>0.963</b>
<b>CORNIAR</b>	<b>0.967</b>	<b>0.964</b>	<b>0.979</b>	<b>0.972</b>	<b>0.979</b>	<b>0.983</b>

approaches, the second two are RR approaches and the remaining are NR approaches. The new corresponding NR approaches, produced through the framework, are called PSNRR, SSIMR, RREDR, WNISM, NIQER, CURVELETR, and CORNIAR as shown in Table 1. It is noted that in the tables and the following tables, the names and results of new NR approaches produced through the response framework are indicated by bold face.

- (2) *The second problem* is to choose some existing IQA approaches for comparison. To evaluate the performances of a new NR approach, a common way is to compare the new NR approach with some FR approaches and state of art NR approaches [9–20, 29]. Generally speaking, FR approaches are easy to implement, and usually provide the accurate and stable image quality assessment; NR approaches are difficult to implement, and have been investigated for years. The chosen IQA approaches include PSNR, SSIM [3], NIQE [10], CURVELET [14], CORNIA [18], BIQI [13], BLIINDS2 [12], BRISQUE [11], IL-NIQE [16] and OG-IQA [20]. The first two are FR approaches and the remaining are NR approaches. Apparently, PSNR, SSIM, NIQE, CURVELET and CORNIA approaches are chosen twice: (1) for the first time, the approaches are chosen for NR approach extension as discussed in the previous paragraph; (2) for the second time, the approaches are chosen for comparison. All the IQA approaches are evaluated according to the Pearson Linear Correlation Coefficient (LCC) and the Spearman Rank Order Correlation Coefficient (SROCC) between predicted quality indexes and subjective quality indexes.

In summary, there are two choices of the existing IQA approaches: one for NR approach extension and the other for NR approach comparison. To keep the paper concise, in the following paragraphs, the “chosen IQA approaches” refer to the IQA approaches for comparison by default.

#### 4.1. Experiments in the LIVE database

The LIVE database contains 29 high-resolution 24bits/pixel RGB color images as reference images and five types of corresponding distorted images: JPEG2000, JPEG, White Noisy (WN), Gaussian blur (GBLUR), and Fast-Fading (FF) Rayleigh channel noisy images [30]. Subjective quality indexes are given in terms of the difference mean opinion score (DMOS) on a scale of 0–100 with a large DMOS indicating poor visual quality. In order to train and test, the database is divided into two subsets, between which there is no overlap. The training subset consists of 80% images, randomly chosen from the LIVE database. The test subset covers the rest 20%. The LCC and SROCC coefficients between predicted quality indexes and subjective quality indexes are employed as criteria for comparison. A value close to 1 for LCC and SROCC indicates superior correlation with human perception. The experimental results are the medians of the indexes across 30 train-test experiments, illustrated in Tables 2 and 3.

In the image response framework,  $\sigma$  in image preprocessing is set to 0.4, 0.6 and 0.8 respectively, and then a test image is transformed into 3 blurred sub-images and 3 enhanced sub-images, namely, 6 image objects.  $\eta$  in image input is set to 0.8, 1.6,  $-0.8$ ,  $-1.6$ , and then there are 8 image inputs to be exerted to each object. In this way, a test image is transformed

**Table 3**

Median SROCCs in the LIVE database.

	JP2K	JPEG	WN	BLUR	FF	ALL
PSNR	0.935	0.931	0.970	0.732	0.896	0.874
SSIM	0.956	0.950	0.967	0.914	0.946	0.916
NIQE	0.777	0.862	0.947	0.703	0.831	0.798
CURVELET	0.884	0.878	0.962	0.925	0.776	0.818
CORNIA	0.901	0.897	0.952	0.952	0.928	0.919
BIQI	0.859	0.717	0.975	0.917	0.768	0.766
BLIINDS2	0.948	0.958	0.964	0.935	0.902	0.923
BRISQUE	0.933	0.934	0.989	0.951	0.876	0.931
IL-NIQE	0.894	0.942	0.981	0.915	0.833	0.902
OG-IQA	0.937	0.964	0.987	0.961	0.899	0.950
<b>PSNRR</b>	<b>0.790</b>	<b>0.762</b>	<b>0.969</b>	<b>0.937</b>	<b>0.742</b>	<b>0.825</b>
<b>SSIMR</b>	<b>0.940</b>	<b>0.928</b>	<b>0.984</b>	<b>0.926</b>	<b>0.872</b>	<b>0.936</b>
<b>WNISMR</b>	<b>0.716</b>	<b>0.608</b>	<b>0.840</b>	<b>0.914</b>	<b>0.752</b>	<b>0.766</b>
<b>RREDR</b>	<b>0.923</b>	<b>0.905</b>	<b>0.958</b>	<b>0.890</b>	<b>0.825</b>	<b>0.927</b>
<b>NIQER</b>	<b>0.948</b>	<b>0.951</b>	<b>0.973</b>	<b>0.945</b>	<b>0.915</b>	<b>0.952</b>
<b>CURVELETR</b>	<b>0.949</b>	<b>0.947</b>	<b>0.988</b>	<b>0.966</b>	<b>0.888</b>	<b>0.953</b>
<b>CORNIAR</b>	<b>0.963</b>	<b>0.953</b>	<b>0.981</b>	<b>0.982</b>	<b>0.981</b>	<b>0.974</b>

into 6 image objects, and each image object produces 8 new NR response features. Consequently, there are 48 response features, which form a global image response feature vector. If each of the features itself consists of  $z$  items, there will be  $48 \times z$  items in the global response vector. Exceptionally, if the features are extended from a NR feature, there will be a NR feature, which is extracted from the test image itself. In this case, the global vector will consist of  $(48 + 1) \times z$  elements. All the features are mapped to a quality index through a three-layer BP neural network, in which there are  $n$ , 400 and 1 nodes in the input layer, hidden layer and output layer respectively.  $n$  is equal to the number (namely,  $48 \times z$  or  $(48 + 1) \times z$ ) of response feature items in the global response feature vector.

From Tables 2 and 3, the following results can be seen from the two tables:

- (1) Through extending the FR (PSNR and SSIM) features to NR features, new NR approaches PSNRR and SSIMR are produced. PSNRR shows no significant differences compared with the existing NR approaches NIQE, CURVELET and BIQI. SSIMR is obviously better than the chosen state of art NR approaches NIQE, CURVELET, CORNIA, BIQI, BLIINDS2, BRISQUE and IL-NIQE except OG-IQA approach. Furthermore, it outperforms the FR approach PSNR, and shows no distinct differences compared with the FR approach SSIM. It can be inferred that both PSNRR and SSIMR can perform well as NR approaches.
- (2) Through extending the RR (WNISM and RRED) features to NR features, new NR approaches WNISMR and RREDR are produced. WNISMR is not ideal, but only slightly inferior to the NR approach NIQE. RREDR performs better than the NR approaches NIQE, CURVELET, BIQI, BLIINDS2, CORNIA and IL-NIQE, and shows no significant differences compared with the FR approach SSIM. It can be inferred that both RREDR and WNISMR can also perform well as NR approaches.
- (3) Through extending the NR (NIQE, CURVELET and CORNIA) features to new NR features, new NR approaches NIQER, CURVELETR, and CORNIAR are produced. The new NR approaches are all superior to the corresponding original NR approaches: NIQER better than NIQE, CURVELETR better than CURVELET and CORNIAR better than CORNIA. Furthermore, they are actually superior to the chosen FR approaches (PSNR and SSIM) and the state of art NR approaches (NIQE, CURVELET, CORNIA, BIQI, BLIINDS2, BRISQUE, IL-NIQE and OG-IQA). CORNIAR achieves the highest LCC and SROCC. It can be inferred that the existing NR approaches are extended to new higher-performance NR approaches. And some of new approaches have superior performance, outperforming SSIM approaches and the state of art NR approaches.

Experimental results show that the response framework is effective to extend existing IQA approaches to new NR approaches. The framework can extend FR approaches and RR approaches to NR approaches, and extend NR approaches to new higher-performance NR approaches. Through extending different image quality feature, different new NR approaches are produced.

#### 4.2. Statistical significance

Tables 2 and 3 show the median LCCs and SROCCs, which present the differences in terms of the median correlation. In this subsection, we evaluate whether the differences in correlation are statistically significant. The standard deviations of LCCs and SROCCs across 30 train-test experiments are tabulated in Tables 4 and 5. Obviously, the performance is better when the median correlation is larger and the standard deviation is lower. From Table 4, it can be calculated that the median standard deviation of the new NR approaches in bold is 0.0211 and the median standard deviation of the chosen approaches (not in bold, including 2 FR approaches and 8 NR approaches) for comparison is 0.0205. Most of all the related standard deviations are smaller than 0.030. There are not significantly different in standard deviation between the new approaches and the chosen approaches. In the same way, the similar result can be drawn from Table 5. Therefore, the medians of the LCC and SROCCs can be used to depict the performance of the IQA approaches.



**Table 4**

Standard deviations of LCCs in the LIVE database.

	JP2K	JPEG	WN	BLUR	FF	ALL
PSNR	0.007	0.014	0.013	0.065	0.026	0.006
SSIM	0.007	0.008	0.010	0.019	0.010	0.003
NIQE	0.020	0.024	0.029	0.042	0.048	0.060
CURVELET	0.038	0.028	0.048	0.030	0.023	0.028
CORNIA	0.020	0.008	0.003	0.006	0.024	0.026
BIQI	0.039	0.031	0.019	0.008	0.027	0.051
BLIINDS2	0.027	0.010	0.006	0.005	0.021	0.024
BRISQUE	0.017	0.010	0.004	0.010	0.028	0.024
IL-NIQE	0.016	0.013	0.006	0.008	0.025	0.023
OG-IQA	0.013	0.008	0.010	0.011	0.022	0.019
<b>PSNRR</b>	<b>0.053</b>	<b>0.029</b>	<b>0.007</b>	<b>0.020</b>	<b>0.047</b>	<b>0.025</b>
<b>SSIMR</b>	<b>0.016</b>	<b>0.017</b>	<b>0.004</b>	<b>0.028</b>	<b>0.022</b>	<b>0.005</b>
<b>WNISMR</b>	<b>0.059</b>	<b>0.079</b>	<b>0.040</b>	<b>0.034</b>	<b>0.018</b>	<b>0.028</b>
<b>RRREDR</b>	<b>0.010</b>	<b>0.022</b>	<b>0.012</b>	<b>0.026</b>	<b>0.037</b>	<b>0.018</b>
<b>NIQER</b>	<b>0.009</b>	<b>0.011</b>	<b>0.007</b>	<b>0.010</b>	<b>0.015</b>	<b>0.017</b>
<b>CURVELETR</b>	<b>0.022</b>	<b>0.020</b>	<b>0.004</b>	<b>0.015</b>	<b>0.052</b>	<b>0.010</b>
<b>CORNIAR</b>	<b>0.009</b>	<b>0.004</b>	<b>0.004</b>	<b>0.007</b>	<b>0.008</b>	<b>0.007</b>

**Table 5**

Standard deviations of SROCCs in the LIVE database.

	JP2K	JPEG	WN	BLUR	FF	ALL
PSNR	0.028	0.027	0.010	0.069	0.025	0.020
SSIM	0.008	0.018	0.004	0.028	0.015	0.014
NIQE	0.022	0.026	0.030	0.038	0.050	0.065
CURVELET	0.042	0.024	0.046	0.030	0.026	0.032
CORNIA	0.023	0.009	0.002	0.006	0.024	0.026
BIQI	0.043	0.037	0.024	0.009	0.038	0.060
BLIINDS2	0.036	0.008	0.007	0.005	0.023	0.025
BRISQUE	0.022	0.013	0.008	0.009	0.027	0.028
IL-NIQE	0.021	0.015	0.009	0.008	0.024	0.022
OG-IQA	0.019	0.010	0.011	0.014	0.022	0.020
<b>PSNRR</b>	<b>0.052</b>	<b>0.039</b>	<b>0.011</b>	<b>0.026</b>	<b>0.040</b>	<b>0.025</b>
<b>SSIMR</b>	<b>0.016</b>	<b>0.022</b>	<b>0.006</b>	<b>0.026</b>	<b>0.020</b>	<b>0.002</b>
<b>WNISMR</b>	<b>0.031</b>	<b>0.084</b>	<b>0.053</b>	<b>0.038</b>	<b>0.035</b>	<b>0.028</b>
<b>RRREDR</b>	<b>0.021</b>	<b>0.015</b>	<b>0.013</b>	<b>0.025</b>	<b>0.045</b>	<b>0.014</b>
<b>NIQER</b>	<b>0.010</b>	<b>0.009</b>	<b>0.010</b>	<b>0.014</b>	<b>0.018</b>	<b>0.024</b>
<b>CURVELETR</b>	<b>0.014</b>	<b>0.025</b>	<b>0.002</b>	<b>0.009</b>	<b>0.069</b>	<b>0.010</b>
<b>CORNIAR</b>	<b>0.008</b>	<b>0.002</b>	<b>0.005</b>	<b>0.010</b>	<b>0.006</b>	<b>0.007</b>

#### 4.3. Relationship between the new NR IQA approaches and their corresponding original existing features

Through the image response framework, the new NR approaches are produced. From Tables 2 and 3, it can be found that the approaches produced based on different existing IQA features shows different performance. This subsection aims to probe into the relationship between the new NR IQA approaches and their corresponding original existing features.

First, investigate the performance of the chosen existing IQA features. The performance of IQA features can be reflected by their corresponding IQA approaches. According to Wang et al. [3], it is concluded that SSIM is better than PSNR; according to Wang and Simoncelli and Soundararajan and Bovik [4, 5], it is concluded that RRRED is better than WNISM; according to Ye et al. and Sun et al. [18, 19], it is concluded that the descending performance order of related NR approaches is: CORNIA, CURVELET and NIQE. From Tables 2 to 5, some similar results can also be arrived. Second, probe into the performance of the new NR IQA approaches. It can found that the performance orders of the new NR approaches are closely related to those of the corresponding original existing IQA approaches: SSIMR is better than PSNRR, RRREDR is better than WNISMR, and the descending performance order of related NR approaches is: CORNIAR, CURVELETR and NIQER. Original existing high-performance IQA features correspond to new high-performance NR approaches. Therefore, it is indispensable to further investigate new high-performance IQA features.

#### 4.4. Algorithm complexity

The approaches produced through the framework consist of three steps: image preprocessing, response feature extraction and quality prediction. In general, for most IQA approaches, the time of image preprocessing and quality prediction is negligible, and the time of response feature extraction takes up most of the running time [4–15]. Consequently, only the time for feature extraction is considered. Firstly, some assumptions are made: the test image is transformed into  $n$  image

**Table 6**

Computation time for the related existing NR approaches.

NIQE	CURVELET	CORNIA	BIQI	BLINDS2	BRISQUE	IL-NIQE	OG-IQA
0.692	2.79	0.83	2.72	115.23	0.28	24.53	0.20

**Table 7**

Computation time for the related new NR approaches.

PSNRR	SSIMR	RREDR	WNISMR	NIQER	CURVELETR	CORNIAR
<b>0.44</b>	<b>5.21</b>	<b>67.12</b>	<b>170.37</b>	<b>35.41</b>	<b>127.18</b>	<b>41.30</b>

objects (sub-images); each image object is exerted with  $m$  inputs; the computational complexity of one response feature extraction from an image object is  $O(\alpha)$ . Then computational complexity of the new NR IQA approach produced through the framework is  $O(nm\alpha)$  (base on existing FR and RR features) or  $O((nm+1)\alpha)$  (based on existing NR features), which indicates that the computational complexity is linear to  $nm$ .

Similarly to computational complexity, the storage requirement of the new NR approach is also linear to  $nm$ . It is supposed that the storage requirement of one response feature from an image object is  $\beta$ , then storage requirement of the new NR IQA approach extended through the framework is  $nm\beta$  (base on existing FR and RR features) or  $(nm+1)\beta$  (based on existing NR features). Fortunately,  $\beta$  is small. For example,  $\beta$  is equal to 8 bytes (one double datum) for existing PSNR and SSIM features. And  $n$  and  $m$  are less than 10. Consequently, the storage requirement is not a tricky problem.

Apparently, it seems that new IQA approaches have high computational complexities. Actually, more new NR approaches are extended from the existing IQA approaches and some of them have small computational complexities. For all the related NR approaches, the computational time of the feature extraction of a test image is tabulated as in Tables 6 and 7. The results are obtained by running an un-optimized matlab program on a 2.67-GHz processor with 4 GB of RAM running Windows 7 and MATLAB R2010a for a  $512 \times 768$  image. Although RREDR, WNISMR, NIQER, CURVELETR and CORNIAR have relatively higher computation complexity, PSNRR has the smallest computational complexity and SSIMR also has a relatively acceptable computation complexity. One would imagine that optimizing the response framework and implementing these approaches efficiently in compilable code (such as C) would further cut down the time needed considerably. It can be predicted that the framework can produce new NR approaches with high accuracy and small computational complexity through further investigation in the near future.

#### 4.5. Database independence

Database independence is to investigate whether the new NR approaches produced through the image response framework are database independent. All the related approaches in Section 4.1 are trained in the LIVE database and then applied to the CSIQ database [31]. There is no overlap between the two databases. The CSIQ database involves 30 original reference color images. Each reference image is degraded using six different types of distortions at four to five different levels of distortion. Subjective quality indexes are provided in terms of DMOS on a scale of 0–1. Among the six types of distortions, JPEG2000, JPEG, additive white noise (WN) and Gaussian blur (GBLUR) are chose for testing, and they are also included in the LIVE database. In the experiments, the training samples come from the LIVE database and the test samples come from the CSIQ database. Apparently, the training samples and the test training samples are the same in each experiment. Consequently, the variances of multiple experimental results are very small and they are mainly caused by the neural network algorithm which is used to map image quality features to quality indexes. Therefore, only the median LCCs and SROCCs are provided across 20 experiments, shown in Tables 8 and 9.

From the two tables, some results can be found as follows:

- (1) The new NR approaches extended from FR and RR approaches are applicable for the CSIQ database except WNISMR. Although WNISMR does not work well, the median of its LCCs/SROCCs coefficients is larger than 0.400, which shows that WNISMR features are valid in some degree. PSNRR and RREDR are not stable in the case that only one type of distorted images is chosen for training and testing. For example, they present high performance for WN distortion, but show relatively low performance for JP2K distortion. However, from overall performance, there are no big differences between the two new NR approaches and the existing approaches NIQE and CURVELET. SSIMR perform well in the CSIQ database. The new NR approach is superior to PSNR and SSIM, and there are only narrow gaps between SSIMR and the state of art NR approaches.
- (2) The new NR approaches NIQER, CURVELETR and CORNIAR, extended from the chosen NR approaches, are all superior to their corresponding original NR approaches NIQE, CURVELET and CORNIA respectively. In other words, the existing NR approaches are improved through the framework. In particular, CORNIAR achieves the best performance and is better than all the chosen FR and NR approaches. All the above results further indicate that the response framework is effective for NR quality assessment.

**Table 8**

Median LCCs in the CSIQ database.

	JP2K	JPEG	WN	BLUR	ALL
PSNR	0.873	0.817	0.938	0.841	0.817
SSIM	0.906	0.908	0.908	0.901	0.833
NIQE	0.832	0.720	0.711	0.713	0.730
CURVELET	0.795	0.679	0.406	0.797	0.747
CORNIA	0.904	0.847	0.742	0.892	0.868
BIQI	0.701	0.851	0.891	0.765	0.801
BLIINDS2	0.887	0.901	0.803	0.848	0.863
BRISQUE	0.826	0.910	0.821	0.873	0.887
IL-NIQE	0.860	0.827	0.870	0.821	0.862
OG-IQA	0.881	0.879	0.871	0.882	0.889
<b>PSNRR</b>	<b>0.649</b>	<b>0.609</b>	<b>0.916</b>	<b>0.693</b>	<b>0.705</b>
<b>SSIMR</b>	<b>0.802</b>	<b>0.872</b>	<b>0.910</b>	<b>0.881</b>	<b>0.835</b>
<b>WNISMR</b>	<b>0.554</b>	<b>0.400</b>	<b>0.377</b>	<b>0.256</b>	<b>0.402</b>
<b>RREDR</b>	<b>0.537</b>	<b>0.833</b>	<b>0.844</b>	<b>0.797</b>	<b>0.720</b>
<b>NIQER</b>	<b>0.855</b>	<b>0.853</b>	<b>0.895</b>	<b>0.918</b>	<b>0.867</b>
<b>CURVELETR</b>	<b>0.697</b>	<b>0.798</b>	<b>0.878</b>	<b>0.893</b>	<b>0.826</b>
<b>CORNIAR</b>	<b>0.938</b>	<b>0.897</b>	<b>0.881</b>	<b>0.942</b>	<b>0.929</b>

**Table 9**

Median SROCCs in the CSIQ database.

	JP2K	JPEG	WN	BLUR	ALL
PSNR	0.896	0.883	0.940	0.878	0.871
SSIM	0.921	0.922	0.926	0.925	0.872
NIQE	0.819	0.745	0.728	0.707	0.736
CURVELET	0.810	0.676	0.448	0.815	0.729
CORNIA	0.890	0.823	0.755	0.901	0.849
BIQI	0.709	0.867	0.880	0.771	0.797
BLIINDS2	0.892	0.895	0.811	0.861	0.872
BRISQUE	0.832	0.924	0.829	0.881	0.876
IL-NIQE	0.858	0.835	0.876	0.814	0.874
OG-IQA	0.892	0.886	0.8705	0.892	0.894
<b>PSNRR</b>	<b>0.636</b>	<b>0.605</b>	<b>0.913</b>	<b>0.786</b>	<b>0.665</b>
<b>SSIMR</b>	<b>0.818</b>	<b>0.889</b>	<b>0.942</b>	<b>0.874</b>	<b>0.852</b>
<b>WNISMR</b>	<b>0.539</b>	<b>0.351</b>	<b>0.398</b>	<b>0.293</b>	<b>0.387</b>
<b>RREDR</b>	<b>0.584</b>	<b>0.840</b>	<b>0.859</b>	<b>0.813</b>	<b>0.734</b>
<b>NIQER</b>	<b>0.850</b>	<b>0.848</b>	<b>0.906</b>	<b>0.917</b>	<b>0.880</b>
<b>CURVELETR</b>	<b>0.711</b>	<b>0.825</b>	<b>0.905</b>	<b>0.894</b>	<b>0.814</b>
<b>CORNIAR</b>	<b>0.941</b>	<b>0.901</b>	<b>0.873</b>	<b>0.948</b>	<b>0.932</b>

## 5. Conclusion

The image response framework is a NR IQA extension framework, through which new NR approaches can be produced. The framework extends the existing FR, RR and NR features to NR response features, equivalent to a process of extending FR, RR and NR approaches to new NR approaches. Experiments show that the new NR approaches extended from the existing FR and RR approaches can perform well as NR approaches; the new NR approaches extended from the existing NR approaches outperform their corresponding original existing NR approaches. Furthermore, some of them are better than FR approaches (PSNR and SSIM) and the state of art NR approaches. The image response framework consists of three aspects: image preprocessing, image inputs and response features. Therefore, there are still a lot of problems deserving further investigation in the novel framework: image preprocessing optimization, image inputs optimization and proper image quality features. Furthermore, it is also worth probing into the response frameworks for the NR quality assessment of video, stereo image and stereo video.

## Acknowledgment

The work is jointly supported by the [National Natural Science Foundation of China](#) (No. 61379101), the [Natural Science Foundation of Jiangsu Province](#) (No. BK20130209), and the [China Postdoctoral Science Foundation](#) (No. 2016M601910).

## References

- [1] Girod B. What's wrong with mean-squared error?. In: Watson AB, editor. *DigitalImage and human vision*. Cambridge, MA: MIT Press; 1993. p. 207–20.
- [2] Wang Z, Bovik AC. Mean squared error: love it or leave it? A new look at signal fidelity measures. *IEEE Signal Process Mag* 2009;26(1):98–117.
- [3] Wang Z, Bovik AC, Sheikh HR, Simoncelli EP. Image quality assessment: from error visibility to structural similarity. *IEEE Trans Image Process* 2004;13(4):600–12.

- [4] Wang Z, Simoncelli EP. Reduced-reference image quality assessment using a wavelet-domain natural image statistic model. In: Proceedings of SPIE—the international society for optical engineering, San Jose, 5666; 2005. p. 149–59.
- [5] Soundararajan R, Bovik AC. RRED indices: reduced reference entropic differencing for image quality assessment. *IEEE Trans Image Process* 2012;21(2):517–26.
- [6] Suthaharan S. Fast communication: No-reference visually significant blocking artifact metric for natural scene images. *Signal Process* 2009;89(8):1647–52.
- [7] Liu H, Klomp N, Heynderickx I. A no-reference metric for perceived ringing artifacts in images. *IEEE Trans Circuits Syst Video Technol* 2010;20(4):529–39.
- [8] Zhu X, Milanfar P. A no-reference sharpness metric sensitive to blur and noise. In: Proc. 1st Int. workshop quality of multimedia experience (QoMEX), San Diego; 2009. p. 64–9.
- [9] Moorthy AK, Bovik AC. Blind image quality assessment: from natural scene statistics to perceptual quality. *IEEE Trans Image Process* 2011;20(12):3350–64.
- [10] Mittal A, Soundararajan R, Bovik AC. Making a completely blind image quality analyzer. *IEEE Signal Process Lett* 2013;20(3):209–12.
- [11] Mittal A, Moorthy AK, Bovik AC. No-reference image quality assessment in the spatial domain. *IEEE Trans Image Process* 2012;21(12):4695–708.
- [12] Saad MA, Bovik AC, Charrier C. Blind image quality assessment: a natural scene statistics approach in the DCT domain. *IEEE Transactions on Image Processing* 2012;21(8):3339–52.
- [13] Moorthy AK, Bovik AC. A two-step framework for constructing blind image quality indices. *IEEE Signal Process Lett* 2010;17(5):513–16.
- [14] Liu L, Dong H, Huang H, Bovik AC. No-reference image quality assessment in curvelet domain. *Signal Process Image Commun* 2014;29(4):494–505.
- [15] Hou W, Gao X, Tao D, Li X. Blind image quality assessment via deep learning. *IEEE Trans Neural Netw Learn Syst* 2014;26(6):1275–86.
- [16] Zhang L, Zhang L, Bovik AC. A feature-enriched completely blind image quality evaluator. *IEEE Trans Image Process* 2015;24(8):2579–91.
- [17] Ye P, Doermann D. No-reference image quality assessment using visual codebooks. *IEEE Trans Image Process* 2012;21(7):3129–38.
- [18] Ye P, Kumar J, Kang L, Doermann D. Unsupervised feature learning framework for no-reference image quality assessment. In: 2012 IEEE conference on computer vision and pattern recognition; 2012. p. 1098–105.
- [19] Sun T, Ding S, Chen W, Xu X. No-reference image quality assessment based on gradient histogram response. *Comput Electr Eng* 2014;54:330–44.
- [20] Liu L, Hua Y, Zhao Q, Huang H, Bovik AC. Blind image quality assessment by relative gradient statistics and adaboosting neural network. *Image Commun* 2015;40(C):1–15.
- [21] Ye P, Kumar J, Kang L, Doermann D. Real-time no-reference image quality assessment based on filter learning. In: IEEE conference on computer vision and pattern recognition IEEE computer society; 2013. p. 987–94.
- [22] Ma L, Li S, Ngan KN. Reduced-reference image quality assessment in reorganized DCT domain. *Signal Process Image Commun* 2013;28(8):884–902.
- [23] Wang S, Jin K, Lu H, Cheng C, Ye J, Qian D. Human visual system-based fundus image quality assessment of portable fundus camera photographs. *IEEE Trans Med Imaging* 2016;35(4):1046–55.
- [24] Ferzli R, Karam LJ. A no-reference objective image sharpness metric based on the notion of just noticeable blur (JNB). *IEEE Trans Image Process* 2009;18(4):717–28.
- [25] Wikipedia. [http://en.wikipedia.org/wiki/Step\\_response](http://en.wikipedia.org/wiki/Step_response).
- [26] Sohn SD, Seong PH. Testing digital safety system software with a testability measure based on a software fault tree. *Reliab Eng Syst Saf* 2006;91(1):44–52.
- [27] Bugalho A, Ferreira D, Barata R, Rodrigues C, Dias SS, Medeiros F, et al. Endobronchial ultrasound-guided transbronchial needle aspiration for lung cancer diagnosis and staging in 179 patients. *Revista Portuguesa De Pneumologia, (English Edition)* 2013;19(5):e1–8.
- [28] Sheikh HR, Bovik AC. Image information and visual quality. *IEEE Trans Image Process* 2006;15(2):430–44.
- [29] Saad MA, Bovik AC, Charrier C. A DCT statistics-based blind image quality index. *IEEE Signal Process Lett* 2010;17(6):583–6.
- [30] Sheikh HR, Sabir MF, Bovik AC. A statistical evaluation of recent full reference image quality assessment algorithms. *IEEE Trans Image Process* 2006;15(11):3440–51.
- [31] Larson EC, Chandler DM. Most apparent distortion: full-reference image quality assessment and the role of strategy. *J Electron Imaging* 2010;19(1):011006.

**Tongfeng Sun** received the Ph.D. degree in detection technology and automation devices from China University of Mining and Technology in 2012. Now he is an associate professor at the School of Computer Science and Technology in the university. His research interests are in the areas of data mining, machine learning and information system.

**Shifei Ding** received his Ph.D. degree from Shandong University of Science and Technology in 2004. And now, he works in China University of Mining and Technology as a professor and Ph.D. supervisor. His research interests include intelligent information processing, pattern recognition, machine learning, data mining and granular computing.

**Xinzheng Xu** received his Ph.D. degree from China University of Mining and Technology in 2012. He is currently an associate professor at School of Computer Science and Technology, China University of Mining and Technology. His research interests include intelligent information processing, pattern recognition, machine learning and granular computing.